PROCEEDINGS OF SCIENCE

The Statistical Properties of ^{92}Mo and Implications for the p-process

Gry Merete Tveten[*a], **A. Spyrou**[b,c,d], **R. Schwengner**[e], **F. Naqvi**[b,d], **A. C. Larsen**[a], **T. Renstrøm**[a], **T. K. Eriksen**[f], **F. L. Bello Garrote**[a], **L. A. Bernstein**[g,h], **D. L. Bleuel**[g], **L. Crespo Campo**[a], **M. Guttormsen**[a], **F. Giacoppo**[i,j], **A. Görgen**[a], **T. W. Hagen**[a], **K. Hadynska-Klek**[k], **M. Klintefjord**[a], **B. S. Meyer**[l], **H. T. Nyhus**[a], **S. J. Rose**[a], **E. Sahin**[a], **S. Siem**[a], **T. G. Tornyi**[f]

[a]*Department of Physics, University of Oslo, Norway*
[b]*National Superconducting Cyclotron Laboratory, Michigan State University, East Lansing, Michigan 48824, USA*
[c]*Department of Physics and Astronomy, Michigan State University, East Lansing, Michigan 48824, USA*
[d]*Joint Institute for Nuclear Astrophysics, Michigan State University, East Lansing, Michigan 48824, USA*
[e]*Helmholtz-Zentrum Dresden-Rossendorf, 01328 Dresden, Germany*
[f]*Department of Nuclear Physics, Research School of Physics and Engineering, The Australian National University, Canberra ACT 2601, Australia*
[g]*Lawrence Livermore National Laboratory, Livermore, California 94551, USA*
[h] *University of California - Berkeley Dept. of Nuclear Engineering, Berkeley CA 94720*
[i] *Helmholtz Institute Mainz, 55099 Mainz, Germany*
[j]*GSI Helmholtzzentrum für Schwerionenforschung, 64291 Darmstadt, Germany*
[k]*INFN, Laboratori Nazionali di Legnaro Padova, Italy*
[l]*Department of Physics and Astronomy, Clemson University, Clemson, SC 29634, USA*
E-mail: g.m.tveten@fys.uio.no

A challenging part of the question of how elements heavier than iron are created in extreme, astrophysical environments is the creation of p-isotopes. The lack of needed nuclear data presents an obstacle in nailing down the precise site and astrophysical conditions for the production of these isotopes. The p-isotope ^{92}Mo represents one of the most severe cases of underproduction. The main destruction mechanism of this isotope in the standard description of the p-process is through the ^{92}Mo(γ, p)^{91}Nb reaction. Measurements on the nuclear level density and γ strength function of ^{92}Mo have been carried out at the Oslo Cyclotron Laboratory. TALYS cross section and reaction rate calculations using the experimental results as input are presented, providing constraints on the ^{91}Nb(p, γ)^{92}Mo (and consequently the inverse) reaction rate. Further, the reaction rates extracted in this work were used in network calculations for the scenario of a p-process taking place in a type II supernova explosion as the shock front passes through the O-Ne layer of a 25 solar mass star. We conclude that there is no salvation in the nuclear input alone in the ^{92}Mo underproduction problem, strengthening previous conclusions pointing towards more exotic astrophysical scenarios.

The 26th International Nuclear Physics Conference
11-16 September, 2016
Adelaide, Australia

1. Introduction

The creation of the so-called p-isotopes remains a puzzling challenge in the quest to explain the production of elements heavier than iron. P-isotopes are stable, proton-rich isotopes that are bypassed by the s- and r-process [1]. Several processes have been suggested to be responsible for producing these nuclei. Currently, these isotopes are commonly believed to be produced in the O-Ne layer of type II supernovae or in type Ia supernovae. In these astrophysical sites the right γ intensities and temperatures could be achievable for photonuclear reactions to erode stable seed nuclei and thereby producing the p-isotopes. Since γ-induced reactions are key to this process it is often also just called the γ-process.

Astrophysical model calculations are able to reproduce abundance patterns of most p-isotopes reasonably well, with some pivotal exceptions. In particular, p-isotopes of mass $92 \leq A \leq 98$ are underproduced in calculations compared to the actual abundance of these isotopes. The p-isotope ^{92}Mo represents one of the most severe cases of underproduction as compared to solar abundances, as illustrated in left panel of figure 1. State-of-the-art p-process calculations systematically underestimate the observed solar abundance of this isotope [1].

The main destruction mechanism of ^{92}Mo in the standard description of the p-process is through the ^{92}Mo(γ, p)^{91}Nb reaction as shown in the right panel of figure 1. This cross section has not yet been determined through direct measurement and has been shown to be a key reaction in sensitivity studies [1, 2]. The nuclear level density (NLD) and γ strength function (γSF) are important inputs to Hauser-Feshbach [3] type calculations as implemented in TALYS [4]. The motivation for this work was to constrain the magnitude of the ^{92}Mo(γ, p)^{91}Nb cross section at relevant energies by obtaining experimental information on the NLD and γSF of ^{92}Mo. The data presented in this work provides stringent constraints on the ^{91}Nb(p, γ)^{92}Mo and its inverse reaction

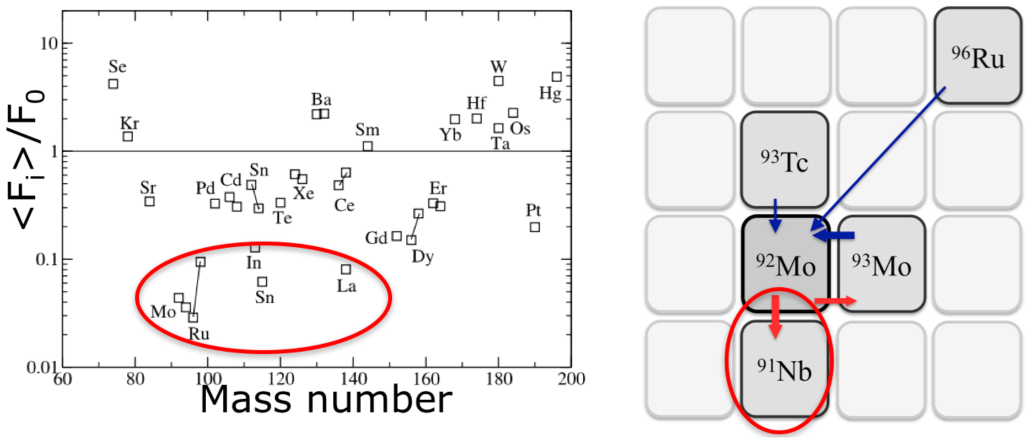

Figure 1: Left panel: This figure illustrates how well the solar abundances of the p-isotopes are reproduced by calculations. If $< F_i > /F_0 = 1$ the calculated isotope abundance value matches solar abundance. The circle indicates the isotopes with the greatest mismatch between calculations and solar abundances. The figure is adopted from reference [1]. Right panel: The main production and destruction mechanisms for ^{92}Mo. The red circle indicates the reaction of main interest. The figure is adopted from reference [5].

*Speaker.

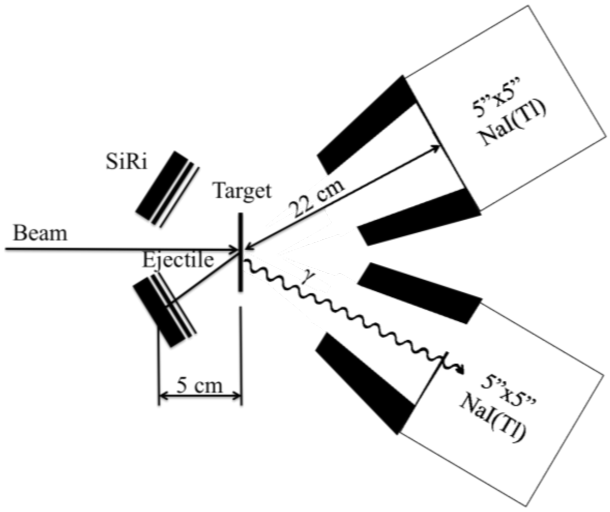

Figure 2: A schematic illustration of the elements of the experimental setup at the Oslo Cyclotron Laboratory.

rate. The astrophysical implications of these constraints are explored in the context of a type II supernova explosion as the shock front passes through the O-Ne layer of a 25 solar mass star. The results presented are presented in reference [5].

2. Experiment and Analysis

Measurements on the NLD and γSF of ^{92}Mo have been carried out at the Oslo Cyclotron Laboratory. The Oslo method is a tool for extracting the NLD and γSF simultaneously from the same data set[6, 7, 8, 9]. The experimental data required for applying the method is γ spectra sorted, event-by-event, as a function of excitation energy, E_x, of the populated compound nucleus. In this work we used a proton beam with 16 MeV kinetic energy that impinged on a self supporting target of isotopically enriched ^{92}Mo. The setup consists of the silicon telescope ring SiRi [10] that allows particle identification and energy measurement, and the NaI scintillator array CACTUS for the γ detection [11]. The setup is shown in figure 2. Particles and γ rays are detected in coincidence. The calibrated γ-ray spectra are unfolded to account for the detector response of the NaI scintillator detectors [8]. The primary γ rays are the first γ rays emitted in a given cascade. The shapes of the primary γ-ray spectra at each E_x are determined by an iterative method where contributions from lower excitation energies are deducted according to a weighting function [6]. It is the matrix of primary γ energies as a function of E_x can be viewed as a probability distribution. The coincidence data and the primary matrice are shown in figure 3. By assuming that the transmission coefficient $\mathscr{T} = \mathscr{T}(E_\gamma)$, in accordance with the generalized Brink-Axel hypothesis [12, 13], the NLD and $\mathscr{T}$ is found according to

$$P(E_\gamma, E_x) \propto \rho(E_x - E_\gamma)\mathscr{T}(E_\gamma). \tag{2.1}$$

where ρ is the NLD. The Oslo method uniquely determines the shape of $\rho(E_x - E_\gamma)$ and $\mathscr{T}(E_\gamma)$, however the equation 2.1 has been shown in reference [6] to have infinitely many solutions that can

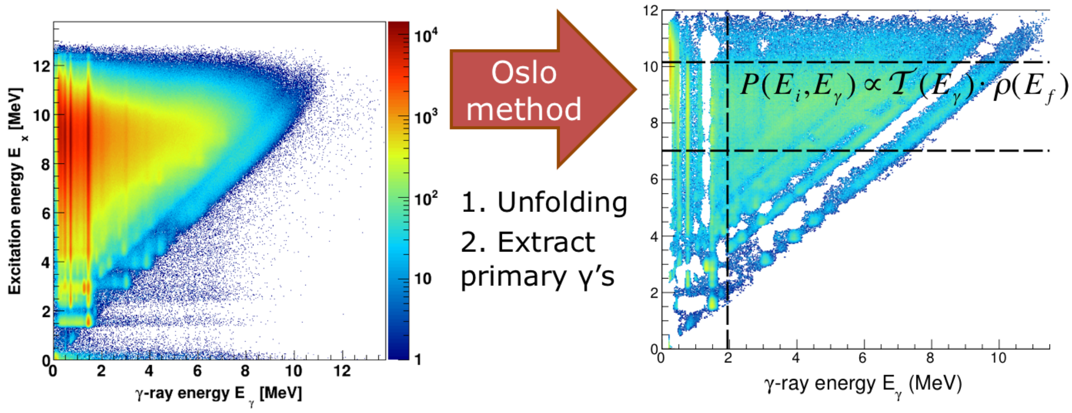

Figure 3: After measuring particle-γ coincidences that are sorted according to E_x (to the left), (1) the γ spectra are unfolded to correct for the detector response and (2) the shape of the primary γ-ray spectra is deduced (to the right). The resulting primary matrix is factorized into a function describing $\rho(E_f)$ and $\mathscr{T}$. Only the part of the landscape assumed to decay in a statistical way is used (limits shown as dashed lines).

be determined through the following transformations

$$\rho(E_x - E_\gamma) = A\exp[\alpha(E_x - E_\gamma)]\rho(E_x - E_\gamma), \tag{2.2}$$

$$T(E_\gamma) = B\exp(\alpha E_\gamma)\mathscr{T}(E_\gamma). \tag{2.3}$$

This entails that the coefficients A, α and B of equations 2.2 and 2.3 must be determined in order to apply the results to cross-section calculations.

The parameters α and A are adjusted so that at low excitation energy our experimental level density reproduces the level density calculated from counting levels measured in discrete spectroscopy. In this case we assumed that the level scheme is complete up to ≈ 4 MeV in accordance with RIPL [14]. At high excitation energy we usually calculate the level density at the neutron binding energy, S_n, from the average resonance spacings. Since ^{91}Mo is uns such data is not available. For ^{92}Mo we estimated $\rho(S_n)$ from the systematics of the Mo-isotopes [14, 15, 16]. Also for the normalization of the γSF, we relied on systematics. In addition to looking at the average radiative width, $\langle\Gamma_\gamma\rangle$, systematics of the Mo-isotopes we required that the γSF in our work can be connected with existing data for other Mo-isotopes for $E_x > S_n$. The γSF is deduced from the transmission coefficent $\mathscr{T}$ by assuming dipole character for contributions to the γSF:

$$f(E_\gamma) = \frac{1}{2\pi}\frac{\mathscr{T}(E_\gamma)}{E_\gamma^3}. \tag{2.4}$$

Measurements on ^{92}Mo are available for the neutron channel for $E_x > S_n$, however the branching to the proton emission channel is significant [17]. Due to the variation in deformation for this isotopic chain, relying on the systematics of the isotopic chain introduces an uncertainty that is challenging to estimate. The error band on the data of this work, shown in figure 4 is the result from normalizing with three sets of normalization parameters to capture the uncertainty in the normalization (see reference [5] for details). The three sets of parameters are given in table 1.

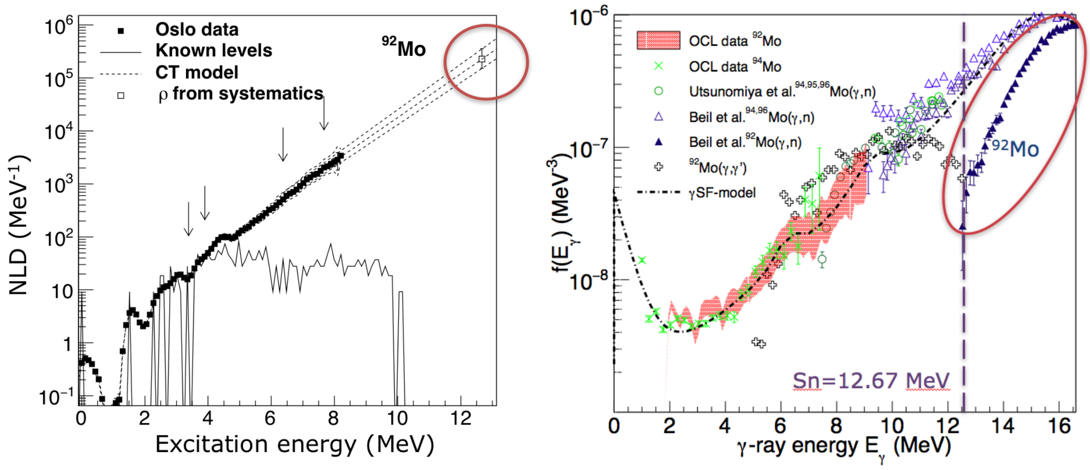

Figure 4: Left panel: The level density extracted in this work. Right panel: The data in this work compared to other measurements and the model used as input to TALYS calculations is shown as a dashed line. The normalization of $f(E_\gamma)$ is uncertain both due to the lack of measurements for resonances at $E_x = S_n$ and because of a significant contribution by the ^{92}Mo(γ, p)-channel. See the text for details.

Parameter	middle	upper	lower
$\rho(S_n)$ (10^5 MeV^{-1})	2.28	3.55	1.52
D_0 (eV)	33	27	48
$\langle\Gamma_\gamma(S_n)\rangle$ (meV)	270	290	250
σ	4.4	5.7	4.2

Table 1: Normalization parameters for $\rho(E_x)$ and $f(E_\gamma)$. $\rho(S_n)$ is the level density at the neutron separation energy and D_0 the corresponding average s-wave resonance spacings that corresponds to for a given spin cutoff parameter, σ, and finally, $\langle\Gamma_\gamma(S_n)\rangle$ is the average radiative width.

3. Astrophysical Reaction Rate Calculations

The astrophysical reaction rates for the ^{91}Nb(p,γ)^{92}Mo reaction were calculated with TALYS 1.6 [4] using input guided by our experimental results for ^{92}Mo. The default global optical model parameters were used for the lower limits [18] and the semi-microscopic nucleon-nucleus spherical optical model (JLM) for the upper limits [19, 20]. The TALYS input for the NLD and γSF for ^{92}Mo were fitted to the experimental NLD and γSF for ^{92}Mo. The generalized Lorentzian model of Kopecky and Uhl [21] with standard RIPL-3 parameters for the GDR strength was used as the starting point. The temperature parameter was chosen to be constant temperature and treated as a free parameter. This temperature was adjusted to fit with both the (γ,n) data displayed in the right panel of figure 4 for $E_x > S_n$ and the data of this work for the γSF below S_n. In addition, two standard Lorentzian resonances (Res 1 and Res 2) were included to replicate the experimental results.

For other Mo-isotopes studied with the Oslo method a low energy enhancement of the γSF has been observed [16, 22]. An exponential function $f(E_\gamma)^{upbend} = C\exp(\eta E_\gamma)$ was adjusted to fit the low energy upbend of the OCL data for ^{94}Mo for completeness. The inclusion of the upbend accounts for $0-3\%$ of the total rate for the relevant temperatures to this work and seems to only

Resonance	Parameter	middle	upper	lower
GDR	E [MeV]	16.04	16.04	16.03
	σ [mb]	188	188	188
	Γ [mb]	4.5	4.6	4.2
	T [MeV]	0.64	0.59	0.59
Res 1	E [MeV]	9.4	9.5	9.4
	σ [mb]	4.7	9.2	3.2
	Γ [mb]	1.5	1.7	1.4
Res 2	E [MeV]	6.3	6.4	6.3
	σ [mb]	0.72	0.79	0.42
	Γ [mb]	0.57	0.76	0.67
Upbend	C [MeV^{-1}]	$4.3{\cdot}10^{-8}$	$4.3{\cdot}10^{-8}$	$4.3{\cdot}10^{-8}$
	η [MeV^{-3}]	-1.9	-1.9	-1.9
CT NLD	T [MeV]	1.10	1.16	1.06
	E_0 [MeV]	0.79	0.64	0.9

Table 2: The resonance and NLD parameters used as input to TALYS 1.6 corresponding to the three different normalizations arrived at in this work (details are given for in table 1).

be an interesting feature for substantially higher temperatures than that assumed to be reasonable for the γ-process ($1.5-3.5$ GK). The total γSF of ^{92}Mo used as input to the TALYS calculations is given by equation 3.1 with the parameters provided in table 2.

$$f(E_\gamma) = f^{GDR} + f^{Res1} + f^{Res2} + f^{upbend} \tag{3.1}$$

The resulting reaction rates calculated with TALYS, as described above, are shown in figure 5. Our experimental constraints on the reaction rates are compatible with the rates of two commonly used data libraries, namely BRUSLIB [23] and JINA-REACLIB [26], as well as most standard options of TALYS. The reaction rate extracted in this work was then used in reaction network calculations for the scenario of a p-process taking place in a type II supernova explosion as the shock front passes through the O-Ne region of a 25 solar mass star. For other reactions than ^{92}Mo(γ, p)^{91}Nb and its inverse, the JINA-REACLIB values were used. The pre-explosive seed distribution of isotopes and a 14 layer division of the O-Ne layer similar to that of reference [1] was used. The reaction network calculations were carried out in the post processing code available in NUCNET tools [25], a suite of nuclear reaction codes developed at Clemson University. The results of these calculations are shown in figure 6. The upper and lower limits shown are the results of varying the JINA-REACLIB rate for ^{92}Mo(γ, p)^{91}Nb up and down with a factor of 3, while the black line corresponds to the cumulative mass fraction of ^{92}Mo using the standard reaction rate. The extracted mass fraction values are slightly below this black line and the result of our work seems to only increase the enigma of ^{92}Mo.

4. Discussion and Outlook

One could argue that it should have been clear from the start that nuclear reaction data only had a minute chance at explaining the underproduction of ^{92}Mo in the context of a shock front

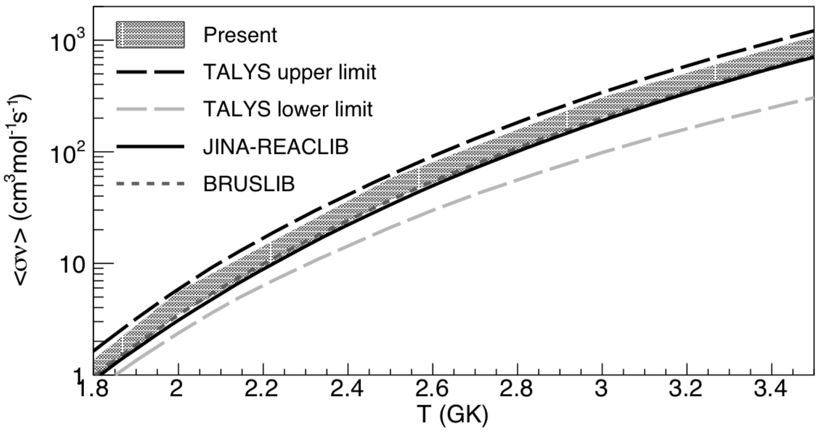

Figure 5: The reaction rates calculated in this work compared to the rates of commonly used libraries. The JINA-REACLIB rate for this particular case is taken from [24]. The figure is adopted from reference [5].

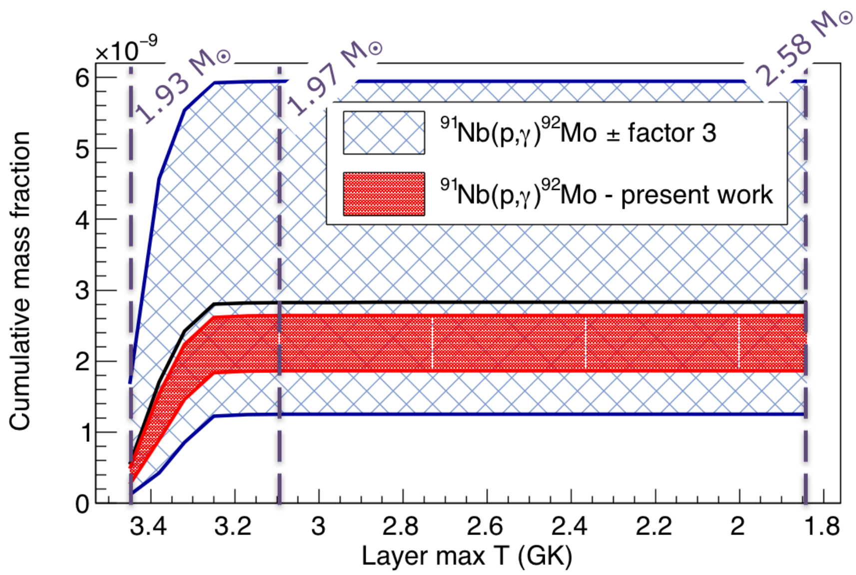

Figure 6: The resulting cumulative mass fractions of ^{92}Mo calculated in this work using the experimental constraints on the NLD and γSF. The horisontal axis gives the maximum temperature in the layers included in the calculations. The upper labels of the figure show the total mass of the star on the inside the layer of a given maximum temperature. The figure is adopted from reference [5].

passing through the O-Ne layer of a massive star. The result of this work strengthens the need to consider other production mechanisms than the γ-process and to scrutinize the details related to the seed nuclei distributions. Nevertheless, the nuclear properties of ^{92}Mo and neighbouring isotopes are interesting to study further also with nucleosynthesis as motivation. Only with precise data input to astrophysical models can various astrophysical scenarious be studied and ruled out. The $N = 50$ isotones are important in the astrophysical context as these isotopes represent bottlenecks due to their low (n,γ) cross sections. Future studies should further explore both the details of the NLD and γSF and bring new insight to this field.

Acknowledgments

We would like to give special thanks to J.C. Müller, A. Semchenkov, and J.C. Wikne for providing the high quality beam and excellent experimental conditions. Lawrence Berkeley National Laboratory is thanked for lending us the ^{92}Mo target. G.M.T. gratefully acknowl- edges funding of this research from the Research Council of Norway, Project Grant No. 222287. A.C.L acknowledges funding from ERC-STG-2014 grant agreement no. 637686. This work was supported by the National Science Foundation under Grants No PHY1102511 (NSCL), No. PHY 1430152 (JINA-CEE) and No PHY 1350234 (CAREER). This work was performed under the auspices of the US Department of Energy DE-AC52-07NA27344 (LLNL) and DE-AC02-05CH11231 (LBNL).

References

[1] W. Rapp, J. Görres, M. Wiescher, H. Schatz and F. Käppeler, The Astrophysical Journal, **653**, 474, (2006).

[2] T. Rauscher *et al.*, MNRAS **463**, 4153-4166 (2016).

[3] W. Hauser and H. Feshbach, Phys. Rev. **87**, 366 (1952).

[4] A. J. Koning and D. Rochman, Nuclear Data Sheets **113** (2012).

[5] G. M. Tveten *et al.*, Phys. Rev. C **94**, 025804 (2016).

[6] A. Schiller *et al.*, Nucl. Instrum. Methods Phys. Res. A **447**, 494 (2000).

[7] A.C. Larsen *et al.*, Phys. Rev. C **83**, 034315 (2011).

[8] M. Guttormsen, T. S. Tveter, L. Bergholt, F. Ingebretsen, and J. Rekstad, Nucl. Instrum. Methods Phys. Res. A **374**, 371 (1996).

[9] M. Guttormsen, T. Ramsøy and J. Rekstad, Nucl. Instrum. Methods Phys. Res. A **255**, 518 (1987).

[10] M. Guttormsen, A. Bürger, T. Hansen and N. Lietaer, Nucl. Instrum. Methods A **648**, 168 (2011).

[11] M. Guttormsen *et al.*, Phys. Scripta T **32**, 54 (1990).

[12] D. Brink, Nucl. Phys. **4**, 215 (1957).

[13] P. Axel, Phys. Rev. **126**, 671 (1962).

[14] RIPL, Nuclear Data Sheets, **110**, 3107 (2009).

[15] P. E. Koehler, A. C. Larsen, M. Guttormsen, S. Siem, and K. H. Guber, Phys. Rev. C **88**, 041305 (2013).

[16] H. Utsunomiya *et al.*, Phys. Rev. C **88**, 015805 (2014).

[17] K. Shoda *et al.*, Nuclear Physics A **239**, 397 (1975).

[18] A. Koning and J. Delaroche, Nuclear Physics A **713**, 231 (2003).

[19] R. Capote *et al.*, Nuclear Data Sheets **110**, 3107 (2009), special Issue on Nuclear Reaction Data.

[20] E. Bauge, J. P. Delaroche, and M. Girod, Phys. Rev. C **58**, 1118 (1998).

[21] J. Kopecky and M. Uhl, Phys. Rev. C **41**, 1941 (1990).

[22] M. Guttormsen *et al.*, Phys. Rev. C **71**, 044307(2005).

[23] M. Arnould and S. Goriely, Nuclear Physics A **777**, 157 (2006), special Issue on Nuclear Astrophysics.

[24] T. Rauscher, Phys. Rev. C **78**, 032801(R) (2008).

[25] B. S. Meyer, NucNet project, (2013)

[26] R. H. Cyburt *et al.*, ApJS **189** 240 (2010).